

# **Spatial patterns of overland flow on disturbed hillslopes**

**Rado Faletic**

Research School of Earth Sciences  
Australian National University  
Canberra 0200

**Dr. Peter Hairsine** (supervisor)  
CRC for Catchment Hydrology  
CSIRO Division of Land and Water  
GPO Box 1666  
Canberra 2601

21<sup>st</sup> February 1997

a report from a vacation scholarship with the CRC for Catchment Hydrology

# Spatial patterns of overland flow on disturbed hillslopes

## Aims

1. To develop a technique for determining the spatial extent of overland flow on disturbed hillslopes from video and photographic images, so as to enable the assessment of contributing area to measurement points.
2. To determine the area runoff and contributing area for one rainfall simulator experiment conducted on a hillslope following woodchipping operations.
3. To test a model of the spatial pattern of overland flow on the snig track component of these experiments.
4. To construct a model of the overland flow below the outlet of a road or track which includes the effect of roughness and spatial variability of infiltration.

## Table of Contents

Background.....	2
Percentage runoff area .....	3
Snig track model.....	5
Plume model .....	7
Conclusions .....	9
References.....	10

## Background

This report describes the process followed and results obtained in a vacation student project aimed at improving the understanding of spatial patterns of overland flow on disturbed hillslopes. This understanding is needed to firstly gain some insight into how water connects through to a drainage line, and if indeed it does connect through. This problem is inherently governed by the spatial variation of properties such as infiltration, soil structure and vegetation. Secondly, to test the predictions of models which rely heavily on point source data. These models may predict realistic results, but how realistic can only be determined upon comparison with any available spatial data.

There are many factors that hinder the measurement of spatial patterns: speed of pattern development, vast amounts of spatial data and the rugged nature of the hillslope environment. Therefore we opted to use images to measure spatial pattern.

The approach that was taken was to firstly obtain and analyse field data, in the form of video and photographs (5 minute intervals) taken vertically above the hillslope area, and secondly some modelling which incorporated the spatial variability of pathways and infiltration rates.

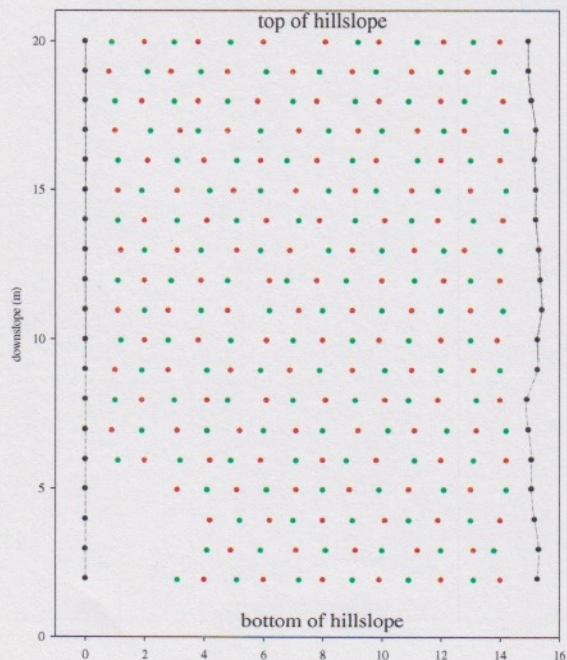


Figure 1a graphical representation of dye bomb positions.

This particular experiment was chosen for this spatial pattern study as is it would minimise obscuring of data by foliage and debris.

The experiment area was covered with dye bombs, placed on a regular 1m x 1m grid (figure 1a). Dye traced the water flow patterns, so they could be recorded on film and video for later analysis. The bombs were alternatively filled with rhodamine (red) and fluorescein (green). Construction of the dye bombs included gauze (figure 1b), which

A 300m<sup>2</sup> rainfall simulation was carried out in compartment 51813 in the Orbost forestry district, Victoria. The simulation was operated at two intensities: the equivalent of a one in ten year event (45 mm hr<sup>-1</sup>), and a one in a hundred year event (70 mm hr<sup>-1</sup>). The site had been logged and burned two weeks prior to the experiment. So, this experiment examined the effect of high intensity rain occurring immediately after logging operations.

This experiment was part of a series of experiments examining runoff and sediment movement in forests for a range of soil types and ranges of times after logging (Croke *et al.* 1997).

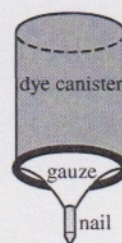


Figure 1b  
dye bomb

ensured that dye would only be released when was ponded on the surface, and therefore the gauze becomes saturated.

### Percentage runoff area

Video and photography were taken from the bucket of a cherrypicker positioned 18m above the site. The data from the photographs was of much superior quality to that from video (Sony Hi8 VideoCam). The video data was used only for qualitative observations. Figure 2a shows an example of the type of view produced by both video and photographs.

The photographs were developed as slides (since slides produce a much higher quality picture) and scanned onto a PC at 1800dpi using Adobe Photoshop 3.0.5 and a Microtek ScanMaker 35t scanner. High colour definition and resolution were needed

since the photographs are from a great distance and taken with a wide-angle lens. The images were then transferred to a Sun Workstation to perform image analysis using a program developed by Chris Moran<sup>1</sup> called *cov\_seg*. This program uses the principle of nearest neighbour in RGB colour space. Colours of interest were identified, such as green/red dye, charcoal and soil, and RGB values for those colours were recorded from pixels which were a 100% representation of that colour. The entire image was then automatically classified into those colour classes. The greatest benefit of this method is that it enhanced the dye streaks whilst suppressing irrelevant data, and



Figure 2a plan view of the general harvest area and snig track.

produced histograms of the various colour classes.

Figures 2b and 2c respectively show the colour histogram and enhanced form of figure 2a, as an example of an image. Often, soil was classified as red dye and charcoal classified as green dye. These errors are due to the dyes being extremely faint in places, so the difference in RGB

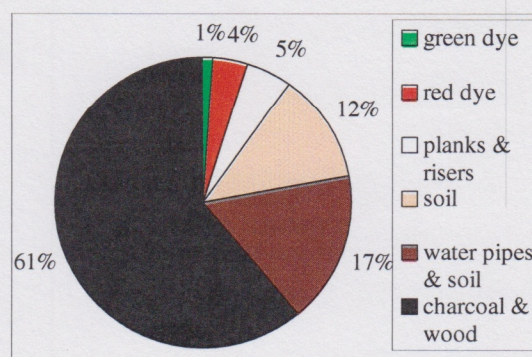


Figure 2b histogram of colour composition of figure 2a.

<sup>1</sup> Huang, J., Moran, C. 1996. 'Determination of soil surface cover using image processing', unpublished.

values of the dye and background surface is very small, hence the classification command has difficulty separating the two similarly coloured objects into different classes. The percentage of red dye in particular is higher on the histogram that is actually present on the hillslope due to this problem – this is visible at the extreme top and bottom of figure 2c.

Colour printouts of the image and its enhancement were made. These were used to sketch the dye streaks onto tracing paper. This was done manually so that interpretation of the actual image, enhanced imaged and sources of error could be made.

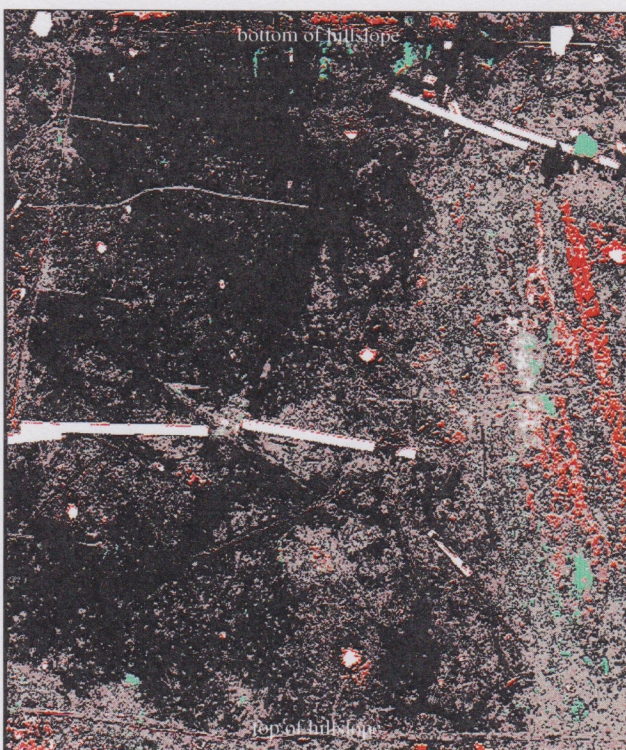


Figure 2c colour classification - plan view.

The area of dye coverage was estimated using the fact that the dye bombs were positioned on a  $1\text{m} \times 1\text{m}$  grid. For every grid element that the dye fell into one square metre was added to the total area covered. Justification for this method is that in most circumstances, water flowing past a dye bomb has a greater width and larger contributing upslope area than is visible from the dye streaks. The estimation of area coverage enabled the time evolution of runoff area (figure 3a) and contributing runoff<sup>2</sup> area (figure 3b) to be examined.

As mentioned above most of the runoff occurred on the snig track. Figures 3c and 3d show the runoff area and contributing runoff area over time for the snig track only. Both figures are very similar, indicating that most of the runoff from the snig track was contributing outflow. These figures are plotted on the same scale as those for the

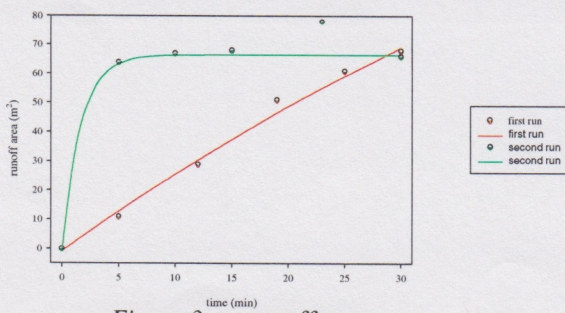


Figure 3a runoff area.

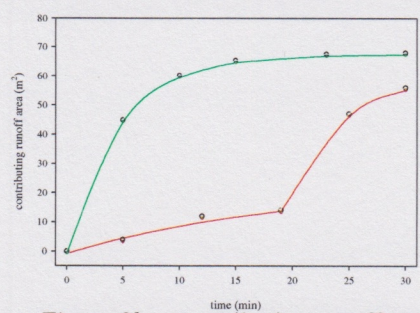


Figure 3b contributing runoff area.

<sup>2</sup> contributing runoff area is the area which contributes runoff to the total outflow of the experiment site.

entire experiment site, so that comparisons between the two can be easily made.

Inspection of the original images shows that dye intensity decreased over time, particularly in the second run. Towards the later part of the second run many of the vibrant green streaks, that were present towards the end of the first run, were no longer visible at all. However, this problem seemed to only effect dye on the general harvest area and not the snig track. Since most of the runoff, as indicated by the dye streaks, was from the snig track this problem did not have a large effect on the results.

The rhodamine was visible in light coloured dirt, such as the snig track, but there is no evidence of it on the general harvest area (charcoal). Conversely, fluorescein was easily visible on the general harvest area but is difficult to see on the lighter snig track.

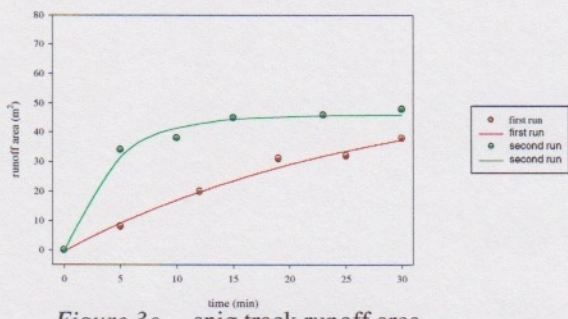


Figure 3c snig track runoff area

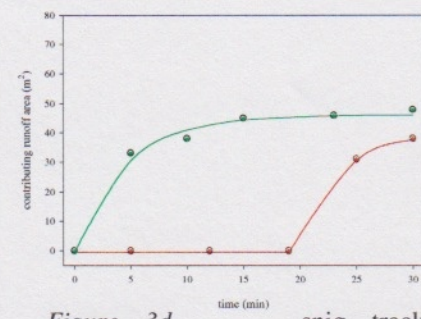


Figure 3d snig track contributing runoff area

The runoff area (figure 3a) shows that the second run reached a steady value early in the run. There is an outlying extreme point at 23 minutes into the run. Therefore is reasonable to assume that the dye intensity began dropping significantly after 23 minutes into the second run. The snig track runoff results show very similar behaviour to those of the whole site, again demonstrating that the snig contributed most of the area to the runoff values.

### Snig track model

Peter Hairsine developed a simple spatial cascade model to examine the spatial behaviour of overland flow, and demonstrate the concept of contributing area. It is based on an  $n \times m$  grid with steady state infiltration, rainfall, parallel flow paths and no autocorrelation between grid cells. The algorithm is as follows ( $x$  is the horizontal grid position and  $y$  is the vertical grid position):

1. Assign infiltration rates randomly.
2. Calculate runoff from topmost cells with no negative runoff allowed  $\rightarrow$   $\text{runoff}(x,1) = \text{rainfall} - \text{infiltration}$ .
3. Calculate runoff from next row of cells (assume a cell runs off to the cell directly below it)  $\rightarrow$   $\text{runoff}(x,2) = \text{runoff}(x,1) + \text{rainfall} - \text{infiltration}$ .
4. Continue until  $\text{runoff}(n,m)$  is calculated.

This model was modified to represent a snig track, incorporating a crossbank at the bottom, and compared with the runoff results obtained from the image data (above). The first three steps in the algorithm remain the same, the rest continues as follows:

4. Continue until  $\text{runoff}(x,y-1)$  is calculated.

5. Calculate runoff from highest point of the crossbank  $\rightarrow$  runoff(1,y) = runoff(1,y-1) + rainfall - infiltration.
6. Calculate runoff from entire crossbank  $\rightarrow$  runoff(x,y) = runoff(x,y-1) + runoff(x-1,y) + rainfall - infiltration.
7. Continue until runoff(n,m) is calculated.

This model assumes exactly the same as the model put forward by Peter Hairsine, with these assumptions extended to the crossbank. The model is a reasonable one to use, as on the experiment site the snig track demonstrated strong parallel flow path behaviour. The infiltration data was therefore chosen so that output from the model was of similar magnitude as that found in the field experiment. Peter Hairsine found that the “percent less than” distribution of infiltration rates is represented well by an a distribution of the form  $100 \times (1 - e^{-\lambda I})$ , where  $\lambda$  is a constant and I is the infiltration rate. The value of  $\lambda$  that was to be used was determine from 1000 runs of the snig track model for many values of  $\lambda$ . The dependence of runoff on  $\lambda$  is shown in figure 4a. From this curve a suitable value of  $\lambda$  was found ( $\lambda = 0.0675$ ).

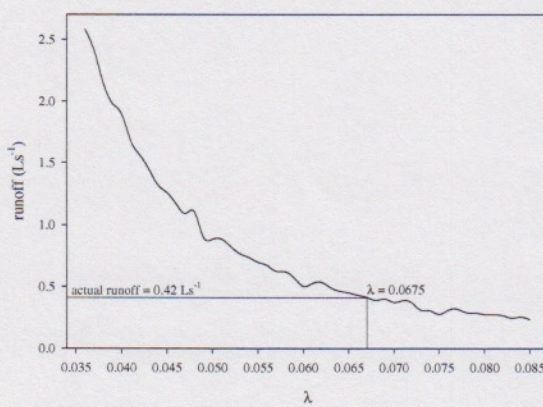


Figure 4a runoff mean versus  $\lambda$ .

This value of  $\lambda$  is much higher than experimental estimates previously suggested for other harvest areas.

Using this value of  $\lambda$  many several simulations were ran, and the spatial pattern of two of them were selected to include in this report, figures 4b and 4c. Both diagrams exhibit typical model behaviour.

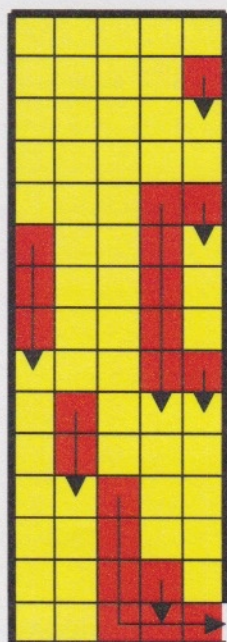


Figure 4b spatial results of the snig track model.

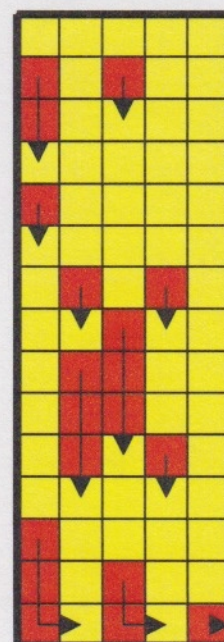


Figure 4c spatial results of the snig track model.

## Plume model

A model of flow from an outlet (plume flow) was constructed, using a hybrid of the snig track model described above and the hillslope flow path model put forward by Quinn *et al.*<sup>3</sup> The new model assigns each grid position with a height and an infiltration rate. The slope on which the model is tested is created with a 15° underlying slope with a random component attached, see figure 5a for an example of this randomness.

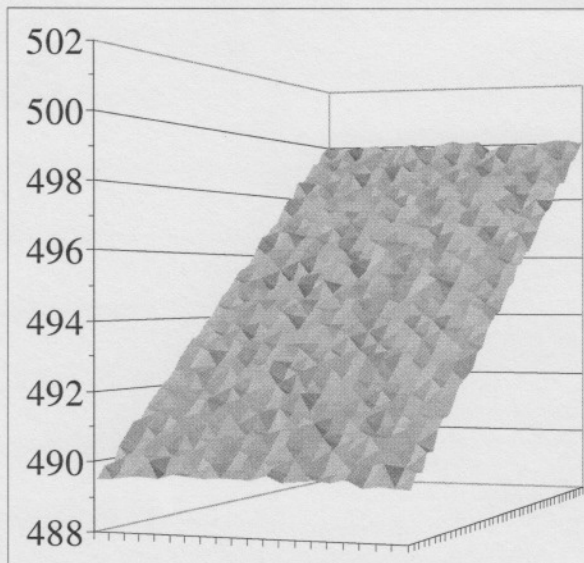


Figure 5a example of the type of hillslope generated by the plume model.

fraction of water must travel in each of the downhill directions (with respect to any cell).

The model was run using several settings: full simulation, rain turned off, infiltration turned off, both rain and infiltration turned off, increased randomness of the terrain. it was found that the increased randomness (from a standard deviation of 0.1m to 0.25m) produced too many depressions in the hillslope, which resulted in the flow travelling only 4-5m before becoming trapped in a depression.

Two examples of the plume model are given here – figure 5c and 5d – which are plots of runoff intensity. Both exhibit a similar behaviour, that of narrow spreading of an intense flow and a wide spread in less significant flow. Before comment can be made about the two diagram it must be noted that models when rain was excluded but infiltration was allowed produced very short flows, the water being infiltrated within a few metres. Also, the scale of both diagrams are different, although the same colouring schemes are employed.

Water input comes from an outlet, and rain. The calculations are carried out much as in the snig track model, although now direction must be taken into account (figure 5b). The directional weighting of flow, proposed by Quinn *et al.*, relies on the difference in height of nearest neighbour cells (where a cell is the area enclosed by the lines of a regular grid), and the direction - lateral or diagonal. This method assumes that water never flows in an uphill direction, which excludes damming and pooling. This is restrictive, particularly if any cell is completely surrounded by cells of greater height.

The model also assumes some

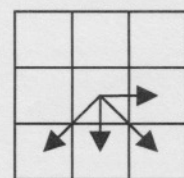


Figure 5b example of possible flow directions.

<sup>3</sup> Quinn, P.F., Beven, K.J., Chevallier, P., and Planchon, O. 1991. 'The prediction of hillslope flow paths for distributed hydrological modelling using digital terrain models', *Hydrological Processes*, 5, 59-79.

These two examples exhibit striking similarity in that the bulk of the runoff is concentrated in a region very close to a straight run downhill. However, the lack in rain, in figure 5d, has lead to a much narrower spread and in all a much less intense run.

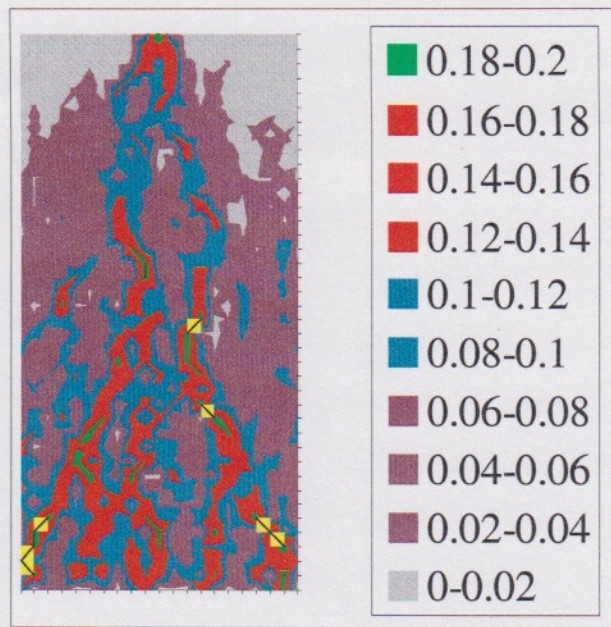


Figure 5b example 1 of the plume model, full simulation with  $\lambda=0.02$  and the rainfall being  $45 \text{ mm hr}^{-1}$  and outlet rate set to  $0.42 \text{ Ls}^{-1}$ .

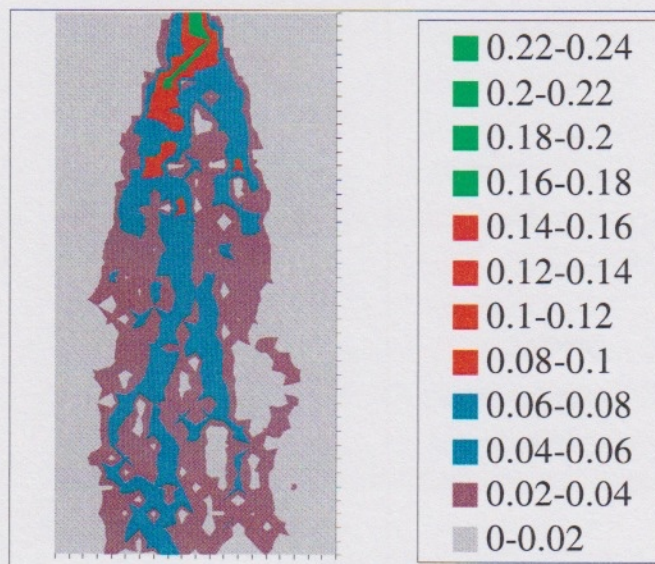


Figure 5c example 2 of the plume model, with no infiltration and no rainfall, and outlet rate set to  $0.42 \text{ Ls}^{-1}$ .

## Conclusions

Although the spatial processes demonstrated here are difficult to analyse by point measurement, a great deal can be found from images and simple numerical models. The image analysis techniques presented here are not new, they have been used by many people for ground cover determination of various materials such as vegetation. The application to spatial development of a system has shown to be a good method for analysis of those spatial processes.

The results from the modelling work presented seem realistic in that the patterns produced are similar to those seen in field sites, particularly the plume model.

## References

- Huang, J., Moran, C. 1996. 'Determination of soil surface cover using image processing', *unpublished*.
- Moore, I.D., Grayson, R.B., and Wilson, J.P. 1990. 'Runoff modelling in complex three-dimensional terrain', *Proceedings of the International Conference on Water Resources in Mountainous Regions, XXII<sup>nd</sup> Congress of the International Association of Hydrologists*, Lausanne, Switzerland, August 27<sup>th</sup> – September 1<sup>st</sup>.
- Morrison Jnr., J.E., Chichester, F.W. 1991. 'Still video image analysis of crop residue soil covers', *Transactions of the ASAE*, **34(6)**, 2469-2473.
- Quinn, P.F., Beven, K.J., and Lamb, R. 1995. 'The  $\ln(a/\tan\beta)$  index: how to calculate it and how to use it within the TOPMODEL framework', *Hydrological Processes*, **9**, 161-182.
- Quinn, P.F., Beven, K.J., Chevallier, P., and Planchon, O. 1991. 'The prediction of hillslope flow paths for distributed hydrological modelling using digital terrain models', *Hydrological Processes*, **5**, 59-79.